J Mater Sci: Mater Electron (2014) 25:2435–2442
DOI 10.1007/s10854-014-1885-3

A model for longitudinal piezoelectric coefficient measurement of the aluminum nitride thin films

Xiaomeng Bi · Yihui Wu · Junfeng Wu · Haiwen Li · Lianqun Zhou

Received: 25 January 2014 / Accepted: 16 March 2014 / Published online: 3 April 2014

Abstract This paper proposes a new model for the longitudinal piezoelectric coefficient (LPC) measurement of the aluminum nitride (AlN) thin film on (100) Si substrate, the AlN thin film is fabricated by the direct-current magnetron sputtering and the piezoelectricity of the AlN thin film is measured by the piezoresponse force microscopy (PFM) in contact mode. In this model, the electric field distribution is taken into account, and the electrostriction displacement caused by the local field concentration is excluded from the measured displacement by the PFM. A LPC value of 4.22 ± 0.34 pm/V is obtained for the clamped AlN thin film by this model, and the deviation between this value and that measured under homogenous field condition is <5.7 %. Therefore, it is reasonable to apply our model to the piezoelectricity characterization of AlN thin films when using the PFM. Furthermore, piezoelectricity of other thin films could also be characterized using this model, which could simplify the measurement process.

X. Bi · Y. Wu (✉) · J. Wu
State Key Laboratory of Applied Optics, Changchun Institute of Optics, Fine Mechanics and Physics, Chinese Academy of Sciences, Changchun 130033, China
e-mail: yihuiwu@ciomp.ac.cn

X. Bi
University of Chinese Academy of Sciences, Beijing 100039, China

H. Li · L. Zhou
Suzhou Institute of Biomedical Engineering and Technology, Chinese Academy of Science, Suzhou 215163, China

1 Introduction

Aluminum nitride (AlN), as one of the III-nitrides, has a wide bandgap, high acoustic velocity, high electrical resistivity, excellent piezoelectricity, good thermal and chemical stability as well as friendly compatibility with traditional IC fabrication process [1, 2]. Due to these outstanding properties, AlN has been widely employed to manufacture electrodevices, such as energy harvesting devices [3, 4], surface acoustic wave (SAW) devices [5–7], thin film bulk acoustic resonators (FBAR) [8, 9], and Lamb wave devices [10], all of which have found their applications in power generation, signal processing and sensing. To improve the performance of these electrodevices, high quality (002) oriented AlN thin films are in demand, for their strong piezoelectricity in the (002) orientation which is along the c-axis direction. AlN films can be fabricated by different techniques, such as metal–organic chemical vapor deposition (MOCVD) [8, 11], molecular beam epitaxy (MBE) [12, 13], pulsed laser deposition (PLD) [14, 15], and reactive magnetron sputtering [6, 16]. Among these techniques, the magnetron sputtering can produce AlN films in mass at a relatively low temperature compatible with the micro-electromechanical systems (MEMS) technology [1]. Therefore, the magnetron sputtering has been widely utilized in the AlN piezoelectric thin film deposition.

As the piezoelectricity of the AlN thin films plays an important role in electrodevices, how to measure the piezoelectric coefficient of the AlN thin films, especially the longitudinal piezoelectric coefficient (LPC) is essential to assess the performance of the AlN film based electrodevices. Two main methods are usually used to measure the piezoelectric coefficient of the AlN thin films, i.e. optical interferometer [17] and piezoresponse force microscopy

(PFM) based on atom force microscopy (AFM) [18–20]. Displacement of top electrode on the AlN thin films is detected by a single-beam optical interferometer, but the substrate would be strained with the expansion and contraction of the AlN film. To decrease the impact of the substrate strain, a double-beam interferometer would be applied with one beam focusing on the top electrode, the other one on the back surface of the substrate. However, strict alignment of the two beams must be satisfied in double-beam method. Comparatively, the PFM technique utilizes a conductive probe, and the tip of probe is in contact with the sample surface. A voltage is applied to the tip, and the piezoelectric displacement is monitored by the tip simultaneously. In the PFM method, the voltage can be applied between the conducting tip and the bottom electrode, or between the top and bottom electrodes [18]. The electric field is homogenous with the voltage applied between the top and bottom electrode, which is of benefit to the determination of piezoelectric coefficient. On the contrary, the electric field is highly inhomogenous when the voltage-applied tip contacts the surface of the AlN film directly. Electric field is concentrated in the contact region, where the electrostrictive effect takes place. Electrostriction displacement would be added into the piezoelectric displacement detected by the PFM, which would lead to errors to the measurement of the piezoelectric coefficient in this case. As far as we know, no research has been done on this issue by now.

In this paper, we utilized a modified tip-film model to measure the LPC of AlN thin film without top electrode by the PFM. The AlN film was deposited on (100) Si substrate by DC magnetron sputtering method, and the crystal structure as well as the surface morphology was investigated by the X-ray diffraction (XRD) and scanning electrical microscope (SEM), respectively. To verify the effectivity of this model, the LPC of the AlN film was also measured under the homogenous-field condition with the voltage applied between the top and bottom electrodes.

2 Method

A voltage is loaded between the tip and the bottom electrode in the measurement of the local LPC of the AlN thin film by the PFM method. The out-of-plane displacement of the AlN thin film is detected via the deflection of the cantilever of the AFM. Combining the measured displacement with the applied voltage V_{tip}, the LPC of the AlN film is usually calculated by the following equation:

$$\Delta t = d_{33}Et = d_{33}V_{tip} \tag{1}$$

where d_{33} is the longitudinal piezoelectric coefficient, $E = V_{tip}/t$ is the electric field in thickness direction and t is the thickness of the film. However, the distribution of the electric field in the thin film beneath the tip is highly inhomogenous, which may induce the error to the piezoelectricity measurement of the AlN thin film. So the nonuniformity of the electric field in (1) should be considered, and the LPC can be calculated under weak electric field condition as in (2),

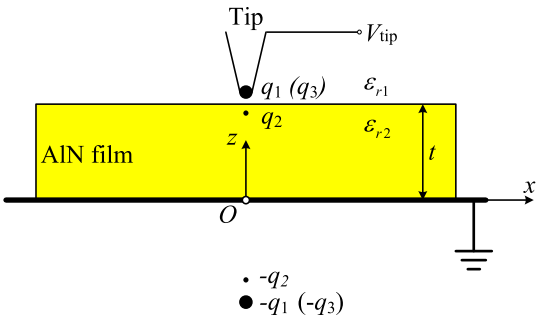

Fig. 1 Schematic of the tip-film configuration. The thickness of the AlN film is t, the equivalent charge of the tip q_1, the induced image charge q_2 with respect to upper surface of AlN as well as their image charges with respect to the bottom electrode $-q_1$, $-q_2$, and these charges are used to calculate the potential and electric field in air via the method of charges; the potential and electric field in AlN film can be obtained by another charge q_3 instead of q_1 and its image charge $-q_3$ by the same method

$$\Delta t = \int_0^t d_{33}\mathrm{E}\cdot\mathrm{n}dz = d_{33}V_{eq} \tag{2}$$

in which **E** is the electric field vector in the AlN film beneath the detected point, **n** is the inward unit normal to the film surface, V_{eq} is the equivalent voltage applied between the tip and the bottom electrode, and the integration is implemented along the film thickness.

In this paper, we use the tip-film system model proposed by *C. Durkan* as shown in Fig. 1 [21], and the tip-film structure is regarded as a capacitance C:

$$C = \frac{2\pi\varepsilon_0 R^2}{t/\varepsilon_{r2} + d/\varepsilon_{r1} + R} \tag{3}$$

where d is the actual tip-surface separation and usually in several angstroms, R is the radius of the tip, ε_{r1} and ε_{r2} are the relative permittivities of the medium above and in the AlN film, respectively, and ε_0 is the permittivity in vacuum. Here, the AlN film is surrounded by the air, so ε_{r1} is assumed to be 1.0. To work out the electric field distribution in the AlN thin film, the voltage-applied tip can be simplified as an equivalent charge $q_1 = CV_{tip}$ with the V_{tip} being the tip applied voltage. By the theory of the image method [22], q_2 is the induced image charge of q_1 with respect to the interface between AlN film and the air, and $-q_1$, $-q_2$ are the image charges of q_1 and q_2 with respect to

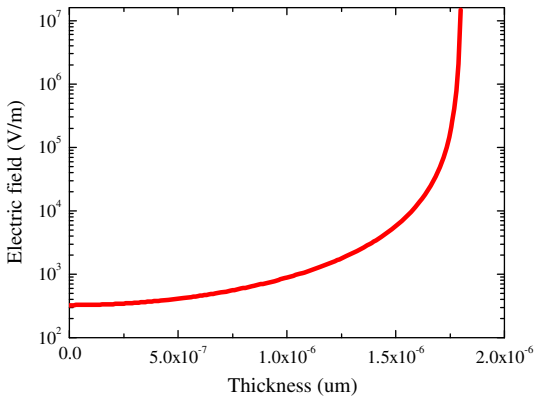

Fig. 2 The electric field distribution of the AlN thin film along the thickness direction beneath the tip with $x = 0$, $d = 0.5$ nm, $R = 40$ nm, $t = 1.8$ μm, $\varepsilon_{r1} = 1.0$, $\varepsilon_{r2} = 9.1$ and $V_{\text{tip}} = 1$ V

the bottom electrode as shown in Ref. [21]. All of these charges are used to calculate the electric potential in the air. In the same way, the electric potential in AlN film is calculated by an equivalent charge q_3 instead of q_1 as well as its image charge $-q_3$ as shown in Fig. 1. The electric potentials $\varphi_{1,2}$ in the two mediums are expressed using the q_1, q_2, q_3 and their image charges as in (4):

$$\begin{aligned}\varphi_1 &= \frac{1}{4\pi\varepsilon_0\varepsilon_{r1}}\left(\frac{q_1}{r_1}+\frac{q_2}{r_2}-\frac{q_2}{r_3}-\frac{q_1}{r_4}\right)\\ \varphi_2 &= \frac{1}{4\pi\varepsilon_0\varepsilon_{r2}}\left(\frac{q_3}{r_1}-\frac{q_3}{r_4}\right)\end{aligned} \tag{4}$$

where r_1, r_2, r_3 and r_4 are the distances from the field point to the charge locations of q_1 (q_3), q_2, $-q_2$ and $-q_1$ ($-q_3$). The electric field $E_{1,2}$ are given in (5):

$$E_{1,2} = -\nabla\varphi_{1,2} \tag{5}$$

Using the boundary conditions at the interface between medium 1 and 2 as well as the zero potential at the bottom electrode, the image charges q_2, q_3 are given in (6) from Ref. [21].

$$\begin{aligned}q_2 &= (1-\varepsilon_{r1}/\varepsilon_{r2})q_1\\ &\quad\times\left[\frac{1/d^{3/2}-1/(t+d)^{3/2}}{1/d^{3/2}-1/(2t+d)^{3/2}}+\frac{1/d^{1/2}-1/(t+d)^{1/2}}{1/d^{1/2}+1/(2t+d)^{1/2}}\right]^{-1}\\ q_3 &= q_1 - q_2\left[\frac{1/d^{1/2}-1/(t+d)^{1/2}}{1/d^{1/2}+1/(2t+d)^{1/2}}\right]\end{aligned} \tag{6}$$

The electric field distribution along the thickness direction of the AlN thin film at $x = 0$ is calculated with $d = 0.5$ nm, $R = 40$ nm, $t = 1.8$ μm, $\varepsilon_{r1} = 1.0$, $\varepsilon_{r2} = 9.1$ [23] and $V_{\text{tip}} = 1$ V in Fig. 2. It can be seen that the electric field in the AlN film increases very slowly with $z < 1.0$ μm, then exponentially increases with z increasing from 1.0 to 1.8 μm and exceeds 10^6 V/m as shown in Fig. 2. In this case, electrostrictive strains would be induced. The electrostriction, which could be neglected in weak electric field, should be considered [24]. Therefore, if the piezoelectric coefficient d_{33} is directly calculated under the homogenous or inhomogenous field in model (1) and (2), the electrostriction displacement may be introduced into the piezoelectric displacement.

To measure the piezoelectric coefficient of the AlN film accurately, both of the electric field distribution and the electrostriction displacement in the film should be taken into account by the following equation:

$$\Delta t = -\int_0^t d_{33}\cdot E_{2z}dz + \int_0^t M\cdot E_{2z}E_{2z}dz \tag{7}$$

where E_{2z} is the component along the z-axis of electric field vector in the AlN thin film and M is the electrostrictive coefficient related to the out-of-plane strain. The first component in the right of (7) is corresponding to the piezoelectric displacement, and the minus is due to the opposite direction of the electric field to that of the z-axis. The second one is the electrostriction displacement. The LPC can be obtained:

$$\Delta t - \int_0^t M\cdot E_{2z}E_{2z}dz\big|_{x=0,y=0} = d_{33}V_{eq} \tag{8}$$

with the equivalent applied voltage $V_{\text{eq}} = -\int_0^t E_{2z}dz$.

3 Experiments

AlN thin films were deposited on the Si (100) substrates by a direct-current (DC) reactive magnetron sputtering instrument (MP500, Plassys Int.co., France). To fabricate AlN films, a 4-inch aluminum target was employed, and the argon and nitrogen were used as the sputtering and the reactive gas, respectively. First of all, the Si substrate was cleaned ultrasonically in acetone, ethanol and deionized water with each step for 5 min, and then the substrate was rinsed with the nitrogen. After the cleaning, the substrate was loaded into the chamber, and the chamber was evacuated to a base pressure of 8.4×10^{-8} Torr. Prior to the deposition of AlN thin film, a titanium layer of 160 nm in thickness was first sputtered onto the Si substrate with a sputtering power of 430 W and Ar flow rate of 30 sccm for 2 min. The sputtering parameters are listed in Table 1. After the AlN thin films were deposited, the sample was kept in the chamber for 1 h at the temperature of 400 °C, which served as annealing process. Then the sample was cooled to room temperature. Aluminum electrodes at four different areas with a diameter of 200 m were patterned on the top of the AlN thin film. The crystal structures of the

Table 1 The sputtering parameters

Parameters	Values
Substrate	(100) Si
Substrate heating temperature	400 °C
Substrate-target distance	75 cm
Targets	4-in 99.999 % pure Al
Sputtering/reactive gases	Ar (99.999 %)/N_2 (99.999 %)
Base pressure	8.4×10^{-8} Torr
AlN sputtering pressure	3.0 mTorr
AlN sputtering power	460 W
Gases flow rate	Ar (3.4 sccm)/N_2 (19.4 sccm) (i.e. 85 % N_2)
Deposition time	4 h

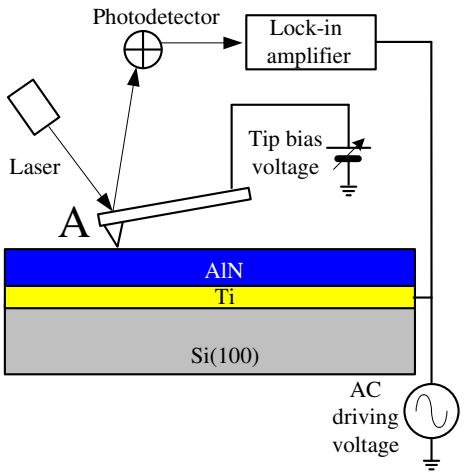

Fig. 3 The schematic diagram of the PFM setup. AC driving and DC bias voltage is applied to the bottom electrode and the tip, respectively. The displacement of the AlN thin film is sensed by the deflection of the cantilever. The deflection signal proportional to the displacement is collected by the photodetector and detected by the lock-in amplifier. The sign of the LPC is dependent on the phase of the deflection signal. If the phase of the deflection signal is in phase with that of the AC applied voltage, the sign is plus, and if the signal is out of phase with that of the AC applied voltage, the sign is minus. The sign of LPC is plus in this paper

AlN thin film were analyzed by XRD (Bruker D8/Discovery) technique, and its surface and cross-sectional morphologies were investigated by SEM (Hitachi S4800).

To characterize the piezoelectricity of the AlN thin films, the PFM method based on the AFM (Multimode VIII, Bruker) was used to measure the out-of-plane displacement of the AlN film in the contact mode using a conductive probe (MESP-HM from Bruker AFM probes, 40 nm in tip radius). Prior to the measurement, the PFM was calibrated by applying a series of known displacements onto the tip. AlN thin film without top electrode were detected by the PFM method as shown in Fig. 3, and the LPC was calculated by different models discussed above. Then to verify the effectivity of the model in this paper, the LPC of the AlN thin film with top electrode was measured.

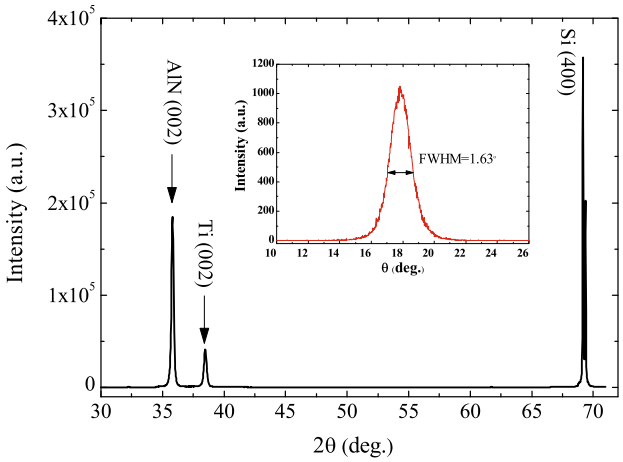

Fig. 4 XRD pattern of the AlN thin film deposited on the (100) Si substrate with Ti bottom electrode at a sputtering power of 460 W, a sputtering pressure of 3.0 mTorr, a nitrogen flow ratio of 85 % as well as substrate heating temperature of 400 °C. The *inset* shows the rocking curve of the (002) orientation of the AlN film

4 Results and discussion

4.1 The AlN piezoelectric thin film deposition

The XRD pattern and the (002) rocking curve (inset) of the AlN thin film are shown in Fig. 4. It demonstrates that only the (002) diffraction peak of the AlN thin film at $2\theta = 36.0°$ is displayed except for the diffraction peaks from the Ti bottom electrode and the Si substrate, which indicates that the AlN thin film has wurtzite structure and grows in c-axis preferred orientation under the sputtering condition listed in Table 1. The full width at half maximum (FWHM) value of the rocking curve is 1.63° from the inset of Fig. 4. It is can be concluded that the c-axis of the deposited AlN thin film is mostly consistent with the normal direction of the substrate.

The surface and cross-sectional morphologies of the AlN thin film are shown in Fig. 5. Pebble-like grains appear on the surface with size ranging from 40 to 200 nm in Fig. 5(a), which is attributed to the extra heating at 400 °C in the chamber after deposition. Heating in the chamber would improve the growth of the crystal grains along the surface, and small grains merge into larger ones as shown in Fig. 5a. Column-structures can be observed in the cross section as shown in Fig. 5b, and the structures are along the normal direction of the surface, which is consistent with the fact that the AlN film grows in (002) oriented direction perpendicular to the substrate surface

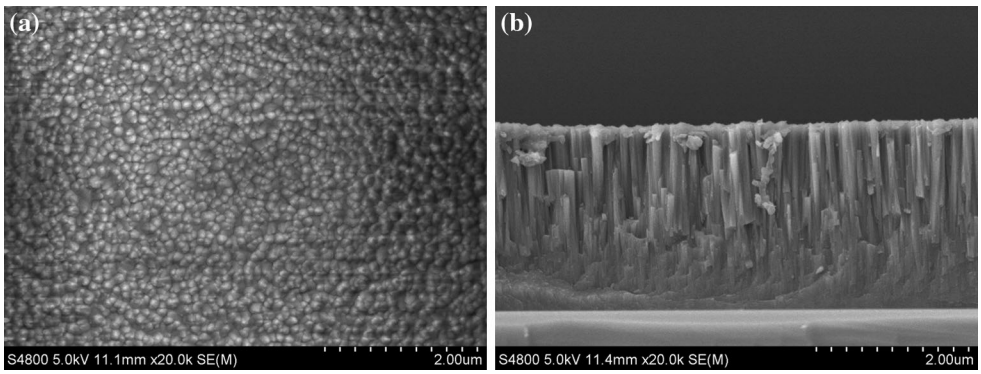

Fig. 5 The surface (**a**) and cross-sectional (**b**) SEM images of the deposited AlN thin film

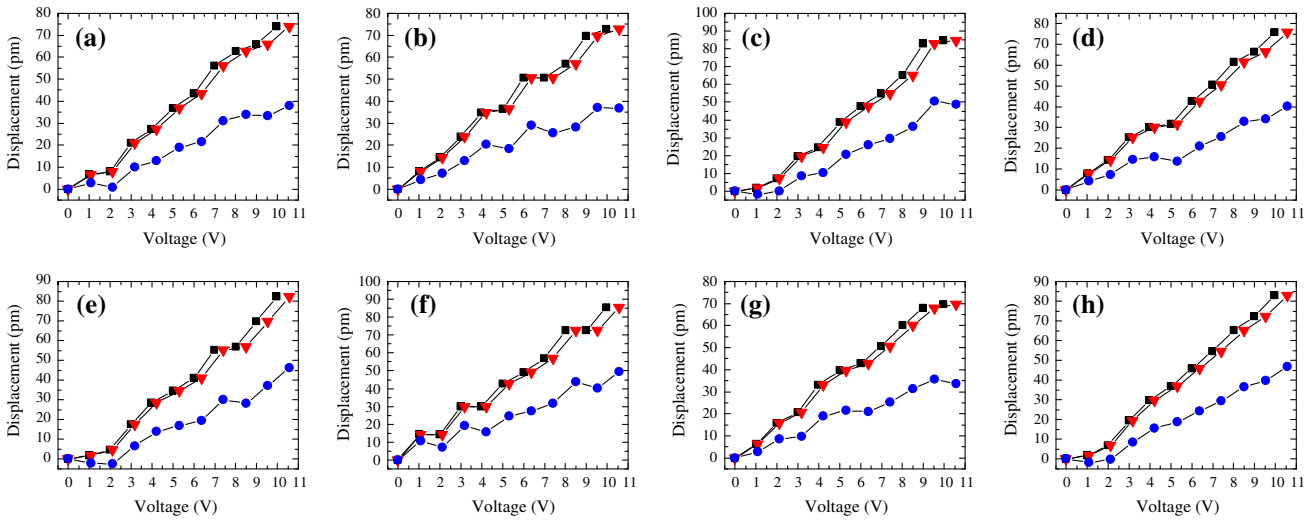

Fig. 6 The displacements of the AlN thin film with the tip bias voltage applied between the tip and the bottom electrode under three different conditions: homogenous field (*square*), only considering nonuniformity of the field (*triangle*) and subtracting the electrostriction component from the detected displacement in the inhomogenous condition (*circular*). **a**–**h** are corresponding to the eight different detected regions

depicted in Fig. 4. The thickness of the AlN thin film is of 1,800 ± 50 nm from the cross-sectional SEM image of the film.

4.2 The measurement of the longitudinal piezoelectric coefficient

The piezoelectric coefficients at eight different detected regions of the AlN thin film were measured by the PFM. The tip bias voltage was increased from 0 to 10.0 V, and the out-of-plane displacements of the AlN were recorded in the same time. The displacements of the AlN thin film versus the voltages under three conditions in (1), (2) and (8) are displayed in Fig. 6, which are corresponding to the measurement done in the homogenous field, inhomogenous field containing the electrostrictive component and ruling out the electrostriction displacement, respectively. The LPC is calculated by the linear fitting of the data, and the results of the LPC are summarized in Table 2. The electrostriction displacements are calculated with the electrostrictive coefficient M to be 0.24×10^{-21} m^2/V^2 [25]. It is shown that the displacements measured under the inhomogenous field in (2) increase with the voltages simultaneously with that under homogenous field in (1), and no obvious deviation can be observed in these two measured condition. The average values of LPC under the homogenous and inhomogenous fields condition are 8.08 ± 0.36 and 7.61 ± 0.34 pm/V, respectively, both of which are larger than the reported value of the AlN thin film [26]. It is useless to just consider the electric field distribution in the AlN thin film. If we subtract the electrostriction displacement from the detected displacement by our modified model, a rational LPC value of 4.22 ± 0.34 pm/V is obtained. It can be seen that the electrostriction displacements account for comparatively large component in the detected displacements, and will be enlarged as the tip bias

Table 2 The piezoelectric coefficient of the AlN thin film without top electrode for different detected areas

Parameters[a]	LPC values for different regions (pm/V)								Average (pm/V)
	(a)	(b)	(c)	(d)	(e)	(f)	(g)	(h)	
d_{33h}^{b}	7.81	7.37	9.26	7.46	8.46	8.29	7.26	8.73	8.08 ± 0.36
d_{33i}^{c}	7.36	6.94	8.72	7.03	7.97	7.81	6.84	8.22	7.61 ± 0.34
d_{33}^{d}	3.97	3.54	5.33	3.64	4.57	4.41	3.44	4.83	4.22 ± 0.34

[a] All the calculated LPC values are for the AlN films clamped on the Si substrate, and values for the bulk materials can be obtained using the method in Ref. [28]

[b] Calculated based on the hypothesis that electric field between the tip and bottom electrode is homogenous

[c] Values calculated in inhomogenous-field condition without excluding the electrostrictive component

[d] Calculated using the model proposed in this paper

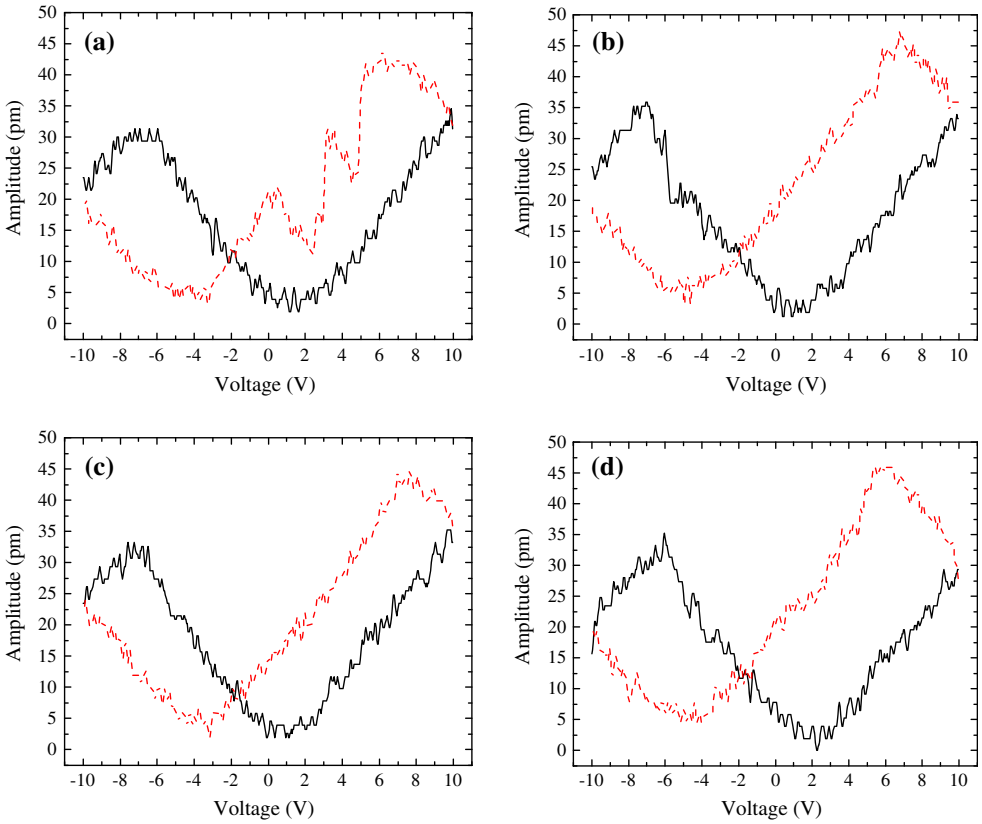

Fig. 7 The piezoresponse of the AlN thin films sandwiched by top and bottom electrodes at different areas of **a**, **b**, **c** and **d**. The amplitude of tip voltage was increased from −10 to 10 V, then back to −10 V with the vibration amplitude of the AlN film recorded meanwhile. The *solid and dash lines* are corresponding to the increasing and decreasing courses, respectively

voltages increase in Fig. 6. Although the displacements increase with the applied voltage, lags are observed in (c), (e) and (h) of Fig. 6 with the applied tip bias voltage <2.0 V, which may be caused by the presence of AlN particles with opposite polarity in the detected region [27]. Additionally, the fluctuation of the displacements in Fig. 6b and f are attributed to the tip location at the grain boundary. The LPC values detected in region (c) are much larger than that in other areas in Table 2, and it is estimated that this is due to the out-of-surface AlN clusters on the surface as shown in Fig. 5a. These clusters are not constrained by the surrounded grains, and free to expand and shrink, so the displacement would be increased when the voltage-applied tip is located on these clusters.

To evaluate the result of our measurement, the LPC value measured by PFM method is first reviewed. Rodriguez et al. [18] reported a $d_{33} = 3.0 \pm 1$ pm/V for AlN/SiC. A LPC value of 5.4 pm/V for AlN thin film on (111) Si substrate and 4.9 pm/V on (100) Si were reported by Tonisch [11] and Mortet [19], respectively. All these values were measured with top electrode patterned on the AlN thin film surface. Shin et al. investigated the piezoelectricity of AlN thin film without top electrode by PFM method and a clamped LPC value of 3.44 pm/V was

accessed [29]. Moreover, the LPC of AlN thin film of 1.7 μm in thickness sandwiched between Ti electrodes was studied by doppler vibrometer, and a value of 2.91 ± 0.31 pm/V for clamped film was obtained [30]. Compared with these reported values, our measured result $d_{33} = 4.22$ pm/V is theoretically reasonable, however, the effectivity of our model can not be confirmed, because of the fact that the piezoelectricity of the AlN thin film is greatly influenced by several factors, such as the fabrication processes [31], thickness of the film [32], oxygen concentration [33], etc. We should bear in mind that the LPC of the AlN thin films deposited under different conditions would vary in values. So a common method should be used for the piezoelectricity characterization of films.

A universal method to measure the LPC of thin films with top electrode in four different areas by the PFM has been utilized [34]. In this method, an AC voltage is applied between the top and bottom electrodes. The amplitude of the applied voltage ramped from −10 to 10 V, and then back to −10 V, meanwhile, the vibration amplitude of the top electrode was recorded. The relationship between the vibration amplitude and the applied voltage amplitude in four different areas is displayed in Fig. 7. Obvious displacement-voltage hysteresis loops are observed. The LPC values in the four top electrode areas are calculated from the slope of the linear parts of the hysteresis loops as the Ref. [34], and a average LPC value of 3.98 ± 0.15 pm/V for the AlN thin film by this method is obtained, which is close to that measured by our modified model with a deviation of 5.7 %. The deviation can be explained that the coefficient values of the AlN thin film sandwiched by electrodes is the global effect across the top electrode, while the values of the AlN thin film without top electrode is just the local piezoresponse of the tip-film contact region. Furthermore, the size and thickness of top electrode as well as the test capacitor feature would influence the measured result [35, 36]. Considering these factors, the deviation between LPC value calculated by our model and that by the universal method is <5.7 %. Therefore, it is proved that it is reasonable to utilize our modified method to measure the LPC of the AlN thin film by the PFM without patterning top electrode.

5 Conclusion

When the PFM is used to measure the longitudinal piezoelectric coefficient of the DC reactive magnetron sputtered AlN thin film without top electrode, the electric field is highly inhomogenous in the film, and electrostrictive effect would take place, which influences the measurement accuracy of the piezoelectric coefficient. In this paper, a modified model has been used to take the distribution of electric field and the electrostriction displacement into account in such case. A value of 4.22 ± 0.34 pm/V has been obtained by this model. To verify our modified model, the piezoelectricity of the AlN thin film has been measured using a common method, i.e. with top electrode patterned on top of the AlN film. It has demonstrated that the deviation between value obtained from our modified model and that from the common method is <5.7 %, which confirms that it is reasonable to use this modified model for the characterization of piezoelectricity of the AlN thin free of patterning top electrode using the PFM method. The modified model can also be used to analyze other piezoelectric thin films without top electrode, which can simplify the measurement process.

Acknowledgments This work was funded by the Natural Science Foundation of China (No. 11034007, 61102023) and the National High Technology Research and Development Program of China (No. 2012AA040503). The authors are grateful to the reviewers for the suggestion and revision of this paper. The authors are grateful to the reviewers for the suggestion and revision of this paper.

References

1. A.V. Singh, S. Chandra, G. Bose, Thin Solid Films **519**, 5846 (2011)
2. K. Tsubouchi, N. Mikoshiba, IEEE Trans. Sonics Ultrason. **32**, 634 (1985)
3. T.T. Yen, H. Taku, K.W. Paul, P.P. Albert, L. Liwei, J. Micromech. Microeng. **21**, 085037 (2011)
4. J. Nathan, O.K. Rosemary, W. Finbarr, O.N. Mike, M. Alan, J. Micromech. Microeng. **23**, 075014 (2013)
5. F. Bénédic, M.B. Assouar, F. Mohasseb, O. Elmazria, P. Alnot, A. Gicquel, Diam. Relat. Mater. **13**, 347 (2004)
6. M. Benetti, D. Cannatà, F. Di Pietrantonio, E. Verona, A. Generosi, B. Paci, V. Rossi, Albertini. Thin Solid Films **497**, 304 (2006)
7. L. Chih-Ming, C. Yung-Yu, V.F. Valery, L. Wei-Cheng, R. Tommi, G.S. Debbie, P.P. Albert, J. Micromech. Microeng. **23**, 025019 (2013)
8. C.M. Yang, K. Uehara, S.K. Kim, S. Kameda, H. Nakase, K. Tsubouchi, IEEE Symp. Ultrason. **1**, 170–173 (2003)
9. J. Weber, W.M. Albers, J. Tuppurainen, M. Link, R. Gabl, W. Wersing, M. Schreiter, Sensor. Actuat. A **128**, 84 (2006)
10. Y. Ventsislav, K. Ilia, J. Micromech. Microeng. **23**, 043001 (2013)
11. K. Tonisch, V. Cimalla, C. Foerster, H. Romanus, O. Ambacher, D. Dontsov, Sensor. Actuat. A **132**, 658 (2006)
12. S. Karmann, H.P.D. Schenk, U. Kaiser, A. Fissel, W. Richter, Mater. Sci. Eng. **50**, 228 (1997)
13. Y. Wu, C.H. Jia, W.F. Zhang, Diam. Relat. Mater. **25**, 139 (2012)
14. H. He, L. Huang, M. Xiao, Y. Fu, X. Shen, J. Zeng, J. Mater. Sci. Mater. Electron. **24**, 4499 (2013)
15. Z.P. Wang, A. Morimoto, T. Kawae, H. Ito, K. Masugata, Phys. Lett. A **375**, 3007 (2011)
16. X.H. Xu, H.S. Wu, C.J. Zhang, Z.H. Jin, Thin Solid Films **388**, 62 (2001)
17. C.M. Lueng, H.L.W. Chan, C. Surya, C.L. Choy, J. Appl. Phys. **88**, 5360 (2000)

18. B.J. Rodriguez, A. Gruverman, A.I. Kingon, R.J. Nemanich, J. Cryst. Growth **246**, 252 (2002)
19. V. Mortet, M. Nesladek, K. Haenen, A. Morel, M. D'Olieslaeger, M. Vanecek, Diam. Relat. Mater. **13**, 1120 (2004)
20. J. Hernando, J.L. Sanchez-Rojas, S. Gonzalez-Castilla, E. Iborra, A. Ababneh, U. Schmid, J. Appl. Phys. **104**, 053502 (2008)
21. M.E. Welland, D.P. Chu, P. Migliorato, Phys. Rev. B **60**, 16198 (1999)
22. J.D. Jackson, *Classical Electrodynamics*, 1st edn. (Wiley, New York, 1962), pp. 26–50
23. X. Song, R. Fu, H. He, Microelectron. Eng. **86**, 2217 (2009)
24. G. Chen, J. Liao, W. Hao, *Fundamental of Crystal Physics*, 2nd edn. (Science Press, Beijing, 2007), pp. 142–144
25. R. Yimnirun, P. Moses, R. Newnham, R. Meyer, J. Electroceram. **8**, 87 (2002)
26. F. Bernardini, V. Fiorentini, Appl. Phys. Lett. **80**, 4145 (2002)
27. A. Sanz-Hervas, M. Clement, E. Iborra, L. Vergara, J. Olivares, J. Sangrador, Appl. Phys. Lett. **88**, 161915 (2006)
28. D. Royer, V. Kmetik, Electron. Lett. **28**, 1828 (1992)
29. S. Hyunchang, T.S. Joon, J. Korean Phys. Soc. **56**, 580 (2010)
30. C.D. Joseph, C.P. Bryan, N. Biju, M. Ravi, L.P. Beth, J. Micromech. Microeng. **20**, 025008 (2010)
31. M.A. Dubois, P. Muralt, J. Appl. Phys. **89**, 6389 (2001)
32. F. Martin, P. Muralt, M.A. Dubois, A. Pezous, J. Vac. Sci. Technol. A **22**, 361 (2004)
33. M. Akiyama, T. Kamohara, K. Kano, A. Teshigahara, N. Kawahara, Appl. Phys. Lett. **93**, 102903 (2008)
34. I.D. Kim, Y. Avrahami, H.L. Tuller, Y.B. Park, M.J. Dicken, H.A. Atwater, Appl. Phys. Lett. **86**, 192907 (2005)
35. W. Zhihong, M. Jianmin, J. Phys. D Appl. Phys. **41**, 035306 (2008)
36. Z. Wang, G.K. Lau, W. Zhu, C. Chao, IEEE. Trans. Ultrason. Ferroelectr. Freq. Control **53**, 15 (2006)